Thermal Fluctuations and Positional Correlations in Oriented Lipid Membranes

T. Salditt,[1] M. Vogel,[2] and W. Fenzl[2]

[1]*Institut für Röntgenphysik, Geiststrasse 11, Universität Göttingen, 37037 Göttingen, Germany*
[2]*Max-Planck Institut für Kolloid- und Grenzflächenforschung, D-14424 Potsdam, Germany*

We have determined the positional correlation functions in aligned stacks of fully hydrated phospholipid bilayers from the thermal diffuse scattering measured by nonspecular x-ray reflectivity. While fair agreement can be obtained between experiment and linear smectic theory at length scales above 120 Å, significant deviations occur at small r, which are tentatively attributed to collective protrusion modes.

Elasticity, thermal fluctuations, and interaction forces of biomimetic lipid membranes in the fluid L_α phase have long been under investigation. Since equilibrium phases of stacked bilayers or multilamellar vesicles with lamellar periodicity d exhibit smectic-A liquid crystalline symmetry, the physical properties are usually discussed in the framework of liquid crystal (LC) physics. The characteristic positional correlation functions in such systems are derived from the linearized smectic free energy functional (Hamiltonian) [1–5],

$$H = \int_A d^2 r \sum_{n=1}^{N-1} \left(\frac{1}{2} \frac{B}{d} (u_{n+1} - u_n)^2 + \frac{1}{2} \kappa (\nabla_{xy}^2 u_n)^2 \right), \quad (1)$$

where κ denotes the bilayer bending rigidity, A the area in the xy plane, N the number of bilayers, and u_n the deviation from the mean average position nd of the nth bilayer. B and $K = \kappa/d$ are elastic coefficients, governing the compressional and bending modes of the smectic phase, respectively. Equation (1) is called the discrete smectic Hamiltonian, in contrast to the continuum (Caillé) model, where the sum over n is replaced by an integral.

As shown by the seminal work of Safinya and co-workers, x-ray scattering and line-shape analysis carried out on aqueous (bulk) suspensions give access to B and $K = \kappa/d$ [2]. For $\kappa \gg kT$, however, which is the typical case for phospholipid systems [6], only the combination of parameters $\sqrt{KB}$ is accessible by measurement of the line-shape exponent $\eta = \pi kT/2d^2\sqrt{KB}$. Moreover, assumptions have to be made on the precise nature of the correlation functions, and it is not possible to assess over which range of length scales the model applies. The main reason for this shortcoming is the loss of information inherent in powder averaging over the unoriented lamellar domains [2].

In this Letter we show that $K(T)$ and $B(T)$ can both be determined independently even for relatively stiff systems $\kappa \gg kT$. Importantly, the analysis does not rely on the characteristic power-law divergence in the vicinity of the Bragg peaks, which is often suppressed by finite size effects [5,7]. We then ask to what extent the linear model

Hamiltonian is applicable to fully hydrated and fluid phospholipid systems. We recall that linear smectic elasticity (with additional surface tension terms) has been extremely successful in describing a series of beautiful quasistatic and dynamic experiments on freestanding films of smectic LC compounds [8,9].

Independent of any specific model, the statistical height-height displacement functions (or correlation function) can be written as $g_{ij}(r) = \langle [u_i(\mathbf{r}') - u_j(\mathbf{r}' + \mathbf{r})]^2 \rangle$. The correlation functions are characterized by two length scales, corresponding (i) to the maximum lateral wavelength of fluctuations ξ_{max} and (ii) the vertical damping length $\Lambda(q_r)$ over which fluctuations of lateral wave number $q_r = \sqrt{q_x^2 + q_y^2}$ are correlated. The two length scales are related: in a film of finite thickness D on a flat substrate, equilibrium fluctuations are excited only on length scales $r \lesssim \xi_{max}$, for which $\Lambda(2\pi/r) \lesssim D$. Thus, on length scales $r \gg \xi_{max}$ the fluctuations are governed by the film interfaces, and the bilayers are essentially flat. Contrarily, on small length scales $r \ll \xi_{max}$ the fluctuations are not affected by the film boundaries and should be described by the bulk Hamiltonian.

From Eq. (1), Lei and co-workers have computed $g_{ij}(r)$ as [4]

$$g_{ij}(r) = \frac{\eta}{\pi^2} d^2 \int_0^\infty dq_{\parallel} \frac{[1 - J_0(q_{\parallel}r)\exp(-\lambda|i-j|dq_{\parallel}^2)]}{q_{\parallel}\sqrt{1 + \frac{Kd^2}{4B}q_{\parallel}^4}},$$
$$(2)$$

with the exponent $\eta = \pi kT/2d^2\sqrt{KB}$ and $\lambda = \sqrt{K/B}$. The height-height self-correlation function $g(r) = g_{ii}(r)$ is of particular interest. Expressed in natural units $R = r/\xi_s$, it can be approximated by $g(R)/(\eta d^2/2\pi^2) = R^2(1.11593 - \ln[R])$ for small $r \lesssim \xi_s$, and by $g(R)/(\eta d^2/2\pi^2) = \ln[R^2] + 1.15443$ for $r \gtrsim \xi_s$. $\xi_s = \sqrt{\lambda d}$ is a crossover length below which the bilayer fluctuates independently from its neighbors. In the limit $r \gtrsim \xi_s$, $g(r)$ diverges logarithmically as is well known from the continuum (Caillé) model [3].

Data have been collected on a well characterized phospholipid system: the zwitterionic, neutral phospholipid

dimyristoyl-sn-glycero-phosphocholine (DMPC, Avanti Lipids, AL). The sample preparation has been described somewhere else [7,10], resulting in an average number of $N \simeq 800$ bilayers with lateral domain sizes in the range of 100 μm and highly oriented with respect to the substrate. The low FWHM $\leq 0.02°$ was preserved after filling the sample chamber with water and swelling the membranes to their equilibrium values in excess water [10]. Thus, in contrast to [7], full hydration was reached.

The experiments were carried out at the undulator beam line ID1 of the ESRF (European Synchrotron Radiation Facility) in Grenoble, using a collimated x-ray beam of 20 keV photon to traverse the 18 mm of bulk water in the temperature-controlled chamber with a 2d multiwire gas detector positioned at 4000 mm behind the sample; see Fig. 1. The angle of incidence was kept constant at $\alpha_i = 0.43° \simeq 5\alpha_c$, placing the specular beam between the two first diffuse Bragg sheets $n = 1, n = 2$ at $2\pi/d$ and $4\pi/d$, respectively, so that no specular Bragg peak was excited.

From the peak positions, a well-defined lamellar periodicity of $d = 64.3$ Å is inferred [11], with a bilayer thickness of about $d_{bl} = 37$ Å. The height-height correlation functions are assessed by evaluating the intensity matrix along the different principal axes, e.g., along the horizontal (Fig. 2) or vertical (Fig. 3) axis. As has been shown previously, the measured diffuse scattering can be written as a unique transformation of the $g_{ij}(r)$ [12].

Horizontal slices, e.g., slices limited by the horizontal dotted lines in Fig. 1, have been evaluated to quantify the decay of the diffuse scattering with q_r for $n = 1, 2$. The integration in q_z (corresponding to the vertical width of the slice) can be increased to approximately cover one Brillouin zone $\pm\pi/d$. In this case, it can be shown that the contributions of the cross-correlation terms $i \neq j$ cancel [13], and one is left with a curve, which corresponds to the transform of an average height-height self-correlation function [7]. The data thus correspond to the averaged structure factor $S(n, q_r)$ of a bilayer in the stack, measured at the order n. In the limit of small $q_z\sigma$ the 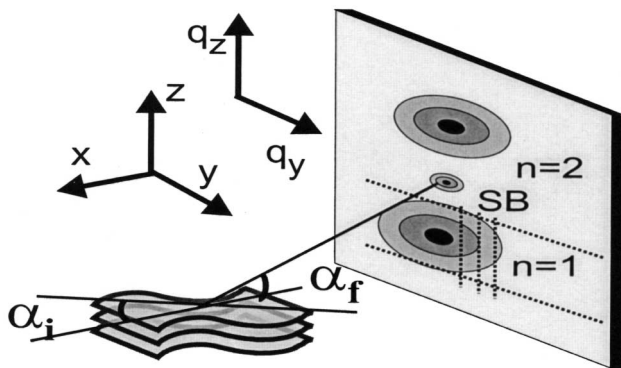curves should overlap for all orders n and be proportional to the bilayer power spectral density (PSD). Here σ denotes the rms-fluctuation amplitude measured over lateral distances ξ_{max}. At finite $q_z\sigma$, the intensity decay still contains the information on the PSD, but is no longer a simple Fourier transform of the PSD [12].

As an example, Fig. 2(a) shows the decay of the integrated intensity with q_r for $n = 1, 2$, respectively, for DMPC at $T = 41.8$ °C. At small $q_r \leq q_r^*$ a plateau is observed, with q_r^* increasing with n. This characteristic shift can be analyzed to determine σ [14]. At high q_r a power-law behavior $S(q_r) \propto q_r^{-\gamma}$ is observed, with $\gamma = 2.71 \pm 0.03$ for the first and $\gamma = 2.70 \pm 0.03$ for the second Bragg sheet, respectively. This is in striking contrast to the $\gamma = 2 - \eta$ behavior expected for a simple logarithmic correlation function $g(r)$ according to linear smectic elasticity theory (continuum model) [3], and also in contrast to an asymptotic $\gamma = 4$ power law, which is the prediction of the discrete smectic model for q_r.

Figure 2(b) shows the result for $g_{exp}(r)$ (open circles) as obtained by numerical back transformation (inversion) [7,15] of the experimental data [in Fig. 2(a)]. In order to perform the transform, the power-law regime in the curves of Fig. 2(a) has to be extrapolated to $q_r \rightarrow \infty$.
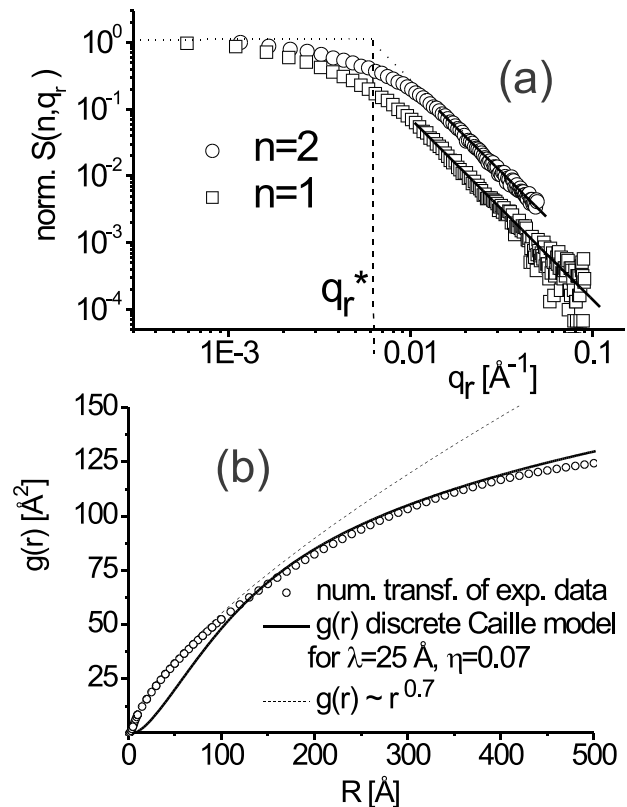

FIG. 2. (a) Horizontal cut through the 2D intensity array, yielding the structure factor $S(n, q_r)$ of an average bilayer along with power-law fits (solid lines), and (b) the corresponding correlation function (open circles) along with $g(r)$ according to Eq. (2) (solid line), as well as an asymptotic power law (dotted line).

FIG. 1. Sketch of the setup with the typical intensity pattern on the 2D detector.

Since the structure factor $S(q_r, q_z \simeq n2\pi/d)$ is not given on an absolute scale, the experimental curve $g_{exp}(r)$ can be determined only up to an arbitrary prefactor. However, the requirement that the transform of both Bragg sheets $n = 1$ and $n = 2$ must give the same function $g_{exp}(r)$ fixes this prefactor and thus the rms amplitude σ of the height fluctuations. Accordingly, the correlation function first increases as $g_{exp}(r) \propto r^{0.71}$, and then saturates for $r \gtrsim \xi_{max} \simeq 600$ Å at $2\sigma^2 \simeq 133 \pm 15$ Å^2, from which a value of $\sigma = 8.1 \pm 0.5$ is obtained. The power-law increase with an exponent of 0.71 can be directly related to the asymptotic behavior of the data in Fig. 2(a), independently confirming the numerical analysis.

We now compare the experimental result $g_{exp}(r)$ to the theoretic prediction of the discrete smectic model $g(r)$. To this end, we must keep in mind that the theoretic form is derived for infinite bulk samples, while the experimental function saturates at a value of $2\sigma^2$ for $r \geq \xi_{max}$, due to finite D. Agreement should therefore be sought only for $r \lesssim \xi_{max}$. A fair degree of overlap between g_{exp} and $g(r)$ is achieved for the parameters $\lambda = 25$ Å and $\eta = 0.072$; see the solid line in Fig. 2(b). Along with d these values correspond to a crossover length of $\xi_s = 40$ Å from independent single bilayer to conformal smectic fluctuations. Note, however, that significant deviations between the experimental and theoretic curves are observed, in particular, at small values $r \simeq \xi_s$. As discussed above, Eq. (2) predicts a power-law regime of $g(r) \propto r^2$ for small $r \lesssim \xi_s$, which crosses over to logarithmic behavior at $r \gtrsim \xi_s$, in contrast to the measured exponents [visible both in the $S(q_r)$ and the $g_{exp}(r)$ curves].

After analysis of the height-height self-correlation, we now turn to the height-height cross correlations, encoded in the q_z profiles of the diffuse Bragg sheets. Figure 3(a) shows a series of cuts through the $n = 1$ Bragg sheet along q_z at constant q_y (DMPC, $T = 41.82$ °C), i.e., along the directions indicated by the vertical dotted lines in Fig. 1, illustrating the peak width (FWHM) and line shape along q_z. The Lorentzian fits (solid lines) indicate an exponential decrease of the cross correlations along z with a characteristic length scale $\Lambda = 2/\text{FWHM}$. The FWHM increases with q_y, reflecting a dependence of the cross-correlation length Λ on the wave number q_r of the height fluctuations or, conversely, the lateral length scale of the fluctuation. Smectic elasticity predicts $\Lambda = 1/(q_r^2\lambda)$. To verify this relationship, we have plotted FWHM versus q_y [16] in Fig. 3(b), along with a least-squares fit to FWHM $= \lambda q_r^2 + \Delta_{res}$, where Δ_{res} accounts for the instrumental resolution. Clearly, we see that the data validate the parabolic relationship and can be analyzed to give the coefficients $\lambda^{1,2}$ for $n = 1, 2$, respectively [17].

The fitting results for $\lambda(T)$ are plotted as a function of T in Fig. 4(a). Note that the gel-fluid phase transition $(P'_\beta \rightarrow L_\alpha)$ appears in the form of a jump in λ. Aside from λ, a second length scale is given by the rms fluctuations of the bilayers. To this end, we evaluate the fluctua-
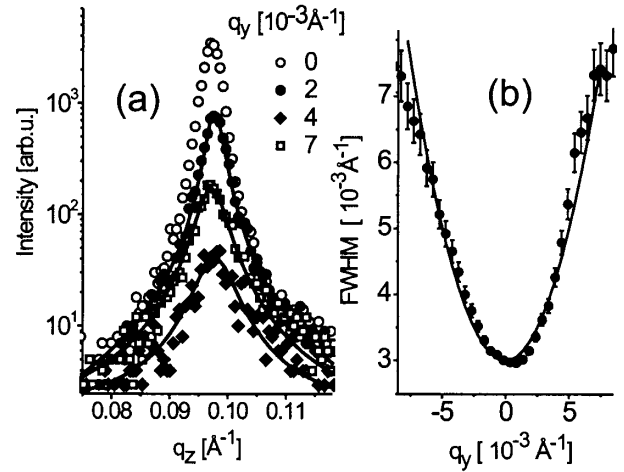

FIG. 3. (a) Cuts through the $n = 1$ diffuse Bragg sheet along q_z at different q_y, showing a characteristic broadening of the q_z width (FWHM), quantified in (b) as a function of q_r, along with a parabolic fit (solid line).

tion amplitude corresponding to the lateral length scale ξ_s, i.e., $\sigma_s^2 := g_{exp}(\xi_s)/2$, shown in Fig. 4(b) as a function of T. The values can be calculated by the back transformation algorithm, or alternatively from the asymptotic form $g_{asy}(r) = cr^{2h}$, which in turn is directly obtained from the measured $S(n = 2, q_r)$ curves [14]. An effective η is then determined from the prefactor needed to scale the theoretic curve $g(r) = (\eta d^2/2\pi^2)G(r)$ to the experimental curve. Specifically, overlap is sought in the range $r \simeq 2d$, where the functional form is found to agree well, in contrast to the systematic deviations at smaller r; see Fig. 2(b), and discussion below. Note that Fig. 4(b) shows the same data points, which can alternatively be read off as σ_s^2 (left axis) or η (right axis), due to the corresponding proportionality. Finally, from λ and the effective parameter η, effective parameters $B(T)$ and $\kappa(T)$ can be calculated directly, as shown in Fig. 4(c). $\kappa(T) \simeq 18kT$ is found to stay approximately constant over the whole range of T in the fluid phase except for a small decrease in the vicinity of the main phase transition $T \simeq 23.5$ °C. Contrarily, B is found to decrease linearly with T in the fluid phase, indicating a corresponding softening of the interbilayer potential with T.

Extrapolating the linear regime to high T, B would vanish around $T \simeq 110$ °C. The decrease in B may be linked to the previously observed transition from a bound state to an unbound state, where the multilamellar membranes detach from the substrate and get dispersed into the aqueous bulk [10]. As a precursor effect to this transition, the interbilayer potential $f(d)$ appears to soften, resulting in a more shallow minimum $B = d_0\partial^2 f/\partial d^2|_{d_0}$.

To our knowledge, this is the first independent measurement of both elasticity coefficients for a pure phospholipid system without softening additives [6]. In contrast to optical measurements, lateral length scales below $\xi_{max} \simeq 600$ Å are probed to determine κ.
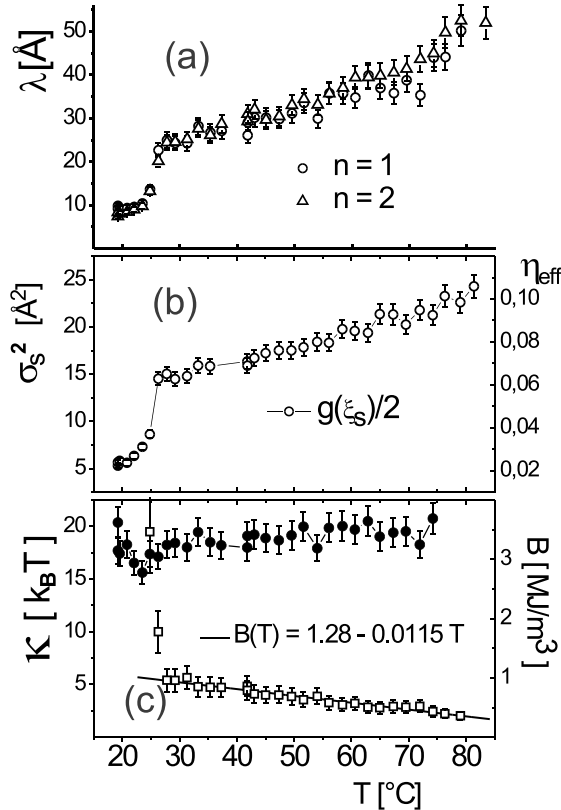
FIG. 4. T dependence of the elasticity coefficients and fluctuation amplitude: (a) $\lambda(T)$, (b) $\sigma_s^2(T)$ or equivalently $\eta(T)$ (right axis), and (c) $\kappa(T)$ (full circles, left axis) and $B(T)$ (open squares, right axis).

However, the derived coefficients have to be regarded as effective parameters, which describe the fluctuation spectrum only partially. Systematic deviations from linear smectic elasticity behavior cannot be overlooked in comparing $g_{\exp}(r)$ to the theoretic curve, in particular, for small r. In this range the fluctuation amplitude is stronger than predicted. This "excess amplitude" may be related to collective modes other than bending, such as protrusion modes or peristaltic modes of the bilayer, which are not contained in Eq. (1). Collective protrusion modes have been studied theoretically [18], and Monte Carlo (MC) simulations have indeed shown that the fluctuation spectrum can be dominated by protrusion modes up to lateral distances of the bilayer thickness [19]. However, in contrast to the crossover from $\gamma = 4$ (independent bilayer regime) to $\gamma = 2$ (collective protrusion) predicted by the single bilayer model of [19], the measured value is $\gamma = 2.7$ for the structure factor of an average bilayer in the multilamellar stack. Further MC simulations could help to understand whether collective protrusions or peristaltic modes can be coupled between adjacent bilayers, and whether this can explain the observed exponent. Note that the present experiment is sensitive to collective bilayer motions, while previous measurements of molecular protrusion by incoherent neutron scattering [20] are insensitive to any collective effects. In summary, we note

that on short length scales phospholipid membrane fluctuations are distinctly different from those of liquid crystalline model compounds [8,9], and that the deviations are probably due to collective protrusion modes. We speculate that these collective molecular motions close to the molecular scale are relevant in biological interactions.

[1] W. Helfrich, Z. Naturforsch. 28C, 693 (1973).
[2] C. R. Safinya et al., Phys. Rev. Lett. 62, 1134 (1989); 57, 2718 (1986).
[3] A. Caillé, C.R. Acad. Sci. B 274, 891 (1972).
[4] L. Ning, C. R. Safinya, and R. Bruinsma, J. Phys. II (France) 5, 1155 (1995); N. Lei, Ph.D. thesis, Rutgers, 1993.
[5] J. Als-Nielsen et al., Phys. Rev. B 22, 312 (1980).
[6] In the absence of surfactants or alcohols (e.g., pentanol).
[7] T. Salditt et al., Phys. Rev. E 60, 7285 (1999).
[8] R. Holyst, D. J. Tweet, and L. B. Sorensen, Phys. Rev. Lett. 65, 2153 (1990); A. C. Price et al., Phys. Rev. Lett. 82, 755 (1999).
[9] E. A. L. Mol et al., Phys. Rev. Lett. 79, 3439 (1997); G. C. Wong et al., Nature (London) 389, 576 (1997); I. Sikharulidze et al., Phys. Rev. Lett. 88, 115503 (2002); A. Fera et al., Phys. Rev. Lett. 85, 2316 (2000).
[10] M. Vogel et al., Phys. Rev. Lett. 84, 390–393 (2000).
[11] d increases from 64.3 Å at $T = 41\,°C$ to $d = 67.5$ Å at $T = 85\,°C$.
[12] S. K. Sinha, E. B. Sirota, S. Garoff, and H. B. Stanley, Phys. Rev. B 38, 2297 (1988); S. K. Sinha, J. Phys. III (France) 4, 1543 (1994).
[13] The diffuse scattering of equivalent interfaces separated by an average distance d is proportional to [12] $S(\mathbf{q}) \propto \sum_{i,j}^{N} e^{-iq_z d(i-j)} \int dr r (e^{q_z^2 c_{ij}(r)} - 1) J_0(q_r r)$, with $c_{ij}(r) = \sigma^2 - g(r, |i - j| d)/2$.
[14] For high $q_z \sigma \geq 1$ or equivalently higher orders n, the structure factor can be approximated by $S(n, q_r) \simeq 2\pi/q_z^2 \int_0^\infty dr r \exp[-q_z^2 g(r)/2] J_0(q_r r)$, with $g(r)$ replaced by the asymptotic expression $g_{asy} = C r^{2h}$ (Eq. 2.19 in [12]). q_r^* can then be calculated for given h [from the slope of $S(n, q_r)$] and compared to the experimental value, e.g., see Fig. 2(a), to determine C. C and h are known, and σ_s is computed from g_{asy}.
[15] T. Salditt, T. H. Metzger, and J. Peisl, Europhys. Lett. 32, 331 (1995).
[16] The q_x component is negligible in the analysis
[17] While the fitted prefactors $\lambda^{(n)}$ depend on the Bragg sheet order n, $\lambda^{(1)}$ can be identified with $\lambda = \sqrt{K/B}$, as can be shown by use of the scattering theory derived in [12]. Furthermore, we find that $\lambda^{(2)} \simeq \lambda^{(1)}/\sqrt{2}$.
[18] R. Lipowsky and S. Grotehans, Biophys. Chem. 49, 27 (1994); Europhys. Lett. 23, 599 (1993).
[19] R. Götz, G. Gompper, and R. Lipowsky, Phys. Rev. Lett. 82, 221 (1999).
[20] S. König, W. Pfeiffer, D. Richter, T. Bayerl, and E. Sackmann, J. Phys. II (France) 2, 1589 (1992).